Printed in the Republic of Korea
ANALYTICAL SCIENCE & TECHNOLOGY
Vol. 35 No. 2, 41-52, 2022
https://doi.org/10.5806/AST.2022.35.2.41

Enhanced ion-exchange properties of clinoptilolite to reduce the leaching of nitrate in soil

John Kabuba★

Department of Chemical Engineering, Vaal University of Technology, Private bag X021, Vanderbijlpark 1900, South Africa

(Received August 19, 2021; Revised November 4, 2021; Accepted December 20, 2021)

Abstract: The leaching of nitrate from soil increases the concentration of elements, such as nitrogen, phosphorus, and potassium, in water, causing eutrophication. In this study, the feasibility of using clinoptilolite as an ion-exchange material to reduce nitrate leaching in soil was investigated. Soil samples were collected from three soil depths (0 − 30, 30 − 90, and 90 − 120 cm), and their sorption capacity was determined using batch experiments. The effects of contact time, initial concentration, adsorbent dosage, pH, and temperature on the removal of NO_3^- were investigated. The results showed that an initial concentration of 25 mg L^{-1}, a contact time of 120 min, an adsorbent dosage of 5.0 g/100 mL, a pH of 3, and a temperature of 30 °C are favorable conditions. The kinetic results corresponded well with a pseudo-second-order rate equation. Intra-particle diffusion also played a significant role in the initial stage of the adsorption process. Thermodynamic studies revealed that the adsorption process is spontaneous, random, and endothermic. The results suggest that a modification of clinoptilolite effectively reduces the leaching of nitrate in soil.

Key words: clinoptilolite, ion exchange, leaching, nitrate, soil

1. Introduction

Nitrogen (N) is a critical nutrient needed in agriculture by plants for growth, and it can be lost in the form of ammonium (NH_4^+) and nitrate through leaching. Nitrate is easily lost because it has a negative charge compared to ammonium ions, which are positively charged and linked to the negative charge of soil. Ammonium ions stored in the soil are readily converted to nitrite, then to nitrate through the nitrification process.[1] This leads to a decrease in the efficient use of nitrogen by plants, limiting crop yield and contributing to environmental pollution. Leaching of nitrate in the soil increases the concentration of elements such as nitrogen (N), phosphorus (P), and potassium (K) in water, causing eutrophication.[2] Nutrients also reach groundwater, which leads to excess dissolved solid such as nitrates in groundwater.[3] NO_3^- can be converted to nitrite in the digestive tracts of infants and ruminant animals, which then combines with blood hemoglobin, reducing its ability to carry oxygen, occasionally leading to death.[4] Nelson *et al*. (2008) used polymer-coated urea to reduce the nitrogen concentration in the soil at the beginning of the season, thereby reducing nitrate leaching. The ability of soil to adsorb anions can reduce NO_3^- leaching and thus play a fundamental role in enhancing soil nutrition.

★ Corresponding author
Phone : +27-(0)16-950-9887 Fax : +27-(0)16-950-9796
E-mail : johnka@vut.ac.za

The application of clinoptilolite into the soil reduces the rate of nitrification because ammonium is absorbed into the clinoptilolite mineral lattice.[6]

Clinoptilolite has been selected as ion-exchange material because it has an extensive application in different fields with its unique properties, such as large specific area, low cost, being eco-friendly, and having a high exchange capacity and microporous structure.[7-9] The presence of aluminium in the structural framework of clinoptilolite results in a negative charge, which is balanced by positively charged cations. These cations are mobile and can be easily charged by other cations-exchange capacity and are unsuitable for anion contaminants. Mažeikiene *et al.* (2008) indicated that clinoptilolite has low nitrate removal efficiency due to the negative charge network at its structure. Its negatively charged aluminosilicate lattice not only attracts different metal cations but can also exhibit an affinity towards anions by suitable modifications. Thus, to enhance the adsorption performance of clinoptilolite, which is appropriate for the elimination of anionic contaminant from aqueous solutions, its surface charge property must be transformed using suitable charge-reversing chemical species.[11] To remove anions, clinoptilolite has to be modified with chitosan. This modification can result in, to a smaller or greater extent, the creation of an adsorption layer on the clinoptilolite surface and the transformation of surface charge on the clinoptilolite surface from negative to positive.[12] Modifying the negatively charged clinoptilolite surface can be conducted by forming layers of adsorbed cationic surfactant, which allows the retention of anions such as nitrate by adsorption. Some modified techniques (Hu *et al.*, 2015) were beneficial to enhance the absorption of nitrate. However, some modifiers had a potential hostile effect on the environment. Chitosan has received vast interest due to its specific characteristics, such as low cost, good adsorption performance, biodegradability, and thus being environmentally friendly, and the presence of the amount of reactive hydroxyl (-OH) and amino ($-NH_2$).[14] This study aims to enhance the ion-exchange properties of clinoptilolite to reduce the leaching of nitrate in soil.

2. Experimental

2.1. Materials

The soil samples were collected from three soil depths (0 – 30, 30 – 90 and 90 – 120 cm) of an uncultivated area in Vanderbijlpark, Gauteng province, South Africa. Pratley Mining Company supplied the natural clinoptilolite used in this study. All the chemicals used were analytical-grade reagents from Sigma-Aldrich Corporation.

2.2. Experimental procedure

The experiment was set up by putting 4 kg of soil in plastic pots. An aliquot of 10 mL of distilled water was added and shaken at 150 rpm for 10 minutes. The time of soil incubation was 50 days. The soil was air-dried and ground to pass a 2 mm sieve. Fertilisation with micro- and macronutrients at a constant level was applied in all the pots. The moisture content of 50 % of the capillary water capacity was maintained throughout the experiment. The soil texture was determined using the hydrometer method. The soil characteristics are provided in *Table* 1.

Exchangeable cations were extracted using the leaching method, with 5 g of soil being placed in a leaching tube (internal diameter = 2 cm; height = 50 cm). A thin layer of glass wool was placed on top of the soil tube to maintain a homogeneous surface during irrigation and leaching studies were done for

Table 1. Physicochemical properties of the soil

OC (%)	N_{total}	pH	HAC	EBC	CEC (m_{eq}/100 g of soil)	BS (%)
0.20	9.33	6.50	11.20	68	80.20	86.73

OC: organic carbon, N_{total}: total nitrogen, HAC: hydrolytic acidity, EBC: total exchangeable cations, CEC: total exchange capacity of soil, BS: basic cations saturation ration in soil

15 days. Afterward, the soil sample was washed with 30 mL of 95 % ethanol. The leachate was collected in a 100 mL volumetric flask, and distilled water was added to make up the volume of a 100 mL volumetric flask. An aliquot of 10 mL of sample from leachate was pipetted into a distillation flask, and 10 mL of 40 % NaOH was added. 10 g of modified clinoptilolite was mixed with 250 mL of synthetic solution and held in a closed polyethylene flask at 90 ºC for 24 hrs. The adsorbents were then separated from the synthetic solution by using a funnel filter. NO_3^- concentration was determined immediately using a spec- trophotometer at 220 nm. The experimental design of the soil leaching experiment was completely randomized design with three replications. Analysis of variance was used to detect treatment effects whereas Tukey's test was used to compare treatment means at $p \leq 0.05$. The Statistical Analysis System version 9.2 was used for the statistical tests. Batch studies were carried out in a 50 mL conical flask of nitrate solution and 200 mg of clinoptilolite. The zeta potential was measured using a Zetasizer Malvern Nano ZS at 25 ºC. The pH of the solution was adjusted to a definite value using HCl and NaOH solutions. To optimize the process, parameters such as pH, adsorbent dosages, contact time, initial concentration, and temperature were investigated. The effect of pH was agreed at the value of 2 – 12, the adsorbent dosage of 0.5 – 5.0 g/100 mL, initial concentration of 25 – 75 mgL^{-1}, temperature at 30 – 50 ºC. Kinetic and isotherm studies were conducted at different nitrate concentrations (25, 50, 75, 100, 125 and 150 mg NO_3^--N L^{-1}). Thermodynamic studies were conducted at 20, 30, 40, and 50 ºC. The equilibrium capacity was calculated using Eq. (1):

Equation (1):

$$q_e = \frac{(C_0 - C_e)}{M} \times V \quad (1)$$

where q_e ($mg.g^{-1}$) is the quantity of nitrate adsorbed at equilibrium, C_e (mg L^{-1}) and C_o (mg L^{-1}) are equilibrium NO_3^--N and initial concentration in aqueous solution, respectively. V (L) is the volume of synthetic solution, and M (g) is the mass of coated clinoptilolite.

2.3. Isotherm models

The Langmuir isotherm model is well described in a linear form, as presented in Eq. (2).[15]

$$\frac{C_e}{q_e} = \frac{C_e}{q_m} + \frac{1}{q_m K_L} \quad (2)$$

where q_m is the amount of ion required to occupy the available site in the unit weight of the solid sample. The Langmuir monolayer adsorption capacity (mg/g), K_L is the Langmuir constant (L/mg). The parameters of the Langmuir model were calculated from the slope-intercept of the plot of C_e/q_e versus q_e. One of the essential characteristics of the Langmuir equation could be expressed by a dimensionless constant, R_L.

$$R_L = \frac{1}{1 + K_L C_o} \quad (3)$$

where C_o is the highest initial solute concentration (mg/L).

The Freundlich isotherm model is described in linear form as seen in Eq. (4).[16,17]

$$log\ q_e = log\ K_F + (1/n)\ log\ C_e \quad (4)$$

where C_e and q_e are the equilibrium concentration (mg/L) and amount adsorbed (mg/g), respectively, and K_F and $1/n$ are Freundlich constants relating to the adsorption capacity and adsorption intensity, respectively. The value of n should be in the range of 1 to 10. The parameters from this model were calculated from the slope-intercept of the plot $log\ q_e$ versus $log\ C_e$.

The Dubinin-Radushkevich isotherm model offers a three-parameter equation, used to represent solute adsorption data on heterogeneous surfaces.[16]

$$ln\ q_e = ln\ q_{max} - k\beta^2 \quad (5)$$

where q_{max} is the D-R monolayer capacity (mg/g), k is the energy constant (mol^2/kJ^2), and β is the Polanyi potential, which is related to the equilibrium concentration defined in Eq. (6).

$$B = RT\ ln\left(1 + \frac{1}{C_e}\right) \quad (6)$$

where R is the gas constant 8.314 in kJ/mol.K, T is

the temperature in K and C_e is the equilibrium concentration in solution (mg/L). The slope of the plot of $ln\ q_e$ versus β gives k (mol^2/kJ^2) and of the intercept yields the adsorption capacity q_{max} (mg/g). The energy required to remove each molecule of metal ions from the solution to the adsorption site can be calculated using Eq. (7).

$$E = \frac{1}{\sqrt{-2K_{ad}}} \quad (7)$$

The value of free energy E is vital and can be obtained in the nature of the adsorption process. If the value of E is ≤ 8 kJ/mol, the adsorption process is physical, but if it is between 8 and 16 kJ/mol, then it can be explained by the ion-exchange mechanism.[14]

2.4. Kinetics of the process

Kinetics is one of the important characteristics defining the efficiency of the process.[18] The study of sorption kinetics provides valuable insights into the reaction pathways and the mechanism of sorption reactions.[19] Before determining the adsorption isotherms, the kinetics of adsorption was studied using three kinetic models:

Pseudo-first order[20]

$$log(q_e - q_t) = log\left((q_e) - \frac{k_1 t}{2.203}\right) \quad (8)$$

Plot: $log\ (q_e - q_t)$ vs. t

Pseudo-second order[21]

$$\frac{t}{q_t} = \frac{1}{K_2 q_e^2} + \frac{1}{q_e} t \quad (9)$$

Plot: $\frac{1}{q_t}$ vs. t

Intraparticle diffusion [22]

$$q_t = k_i t^{1/2} + C_i \quad (10)$$

Plot: q_t vs. $t^{1/2}$

where k_1 is the pseudo-first-order rate constant (1/min), k_2 is the pseudo-second-order rate constant (g/mg.min), k_i is the intraparticle diffusion rate constant ($mg/g.min^{1/2}$), and C_i is the intercept directly proportional to the thickness of the boundary layer (mg/g).

2.5. Thermodynamic studies

In the present study, thermodynamic parameters such as Gibb's free energy change ($\Delta G°$), enthalpy change ($\Delta H°$) and entropy change ($\Delta S°$) were calculated using Eqs. (11), (12), (13) and (14).

$$ln\ K_d = \frac{\Delta S^o}{R} - \frac{\Delta H^o}{RT} \quad (11)$$

$$\Delta G^o = \Delta H° - T\Delta S° \quad (12)$$

$$\Delta G^o = -RT\ ln\ K_d \quad (13)$$

where K_d is the distribution coefficient (mLg^{-1}), R is the universal gas constant (8.314 $Jmol^{-1}/K$), and T is the temperature (ºK).

$$K_d = \frac{q_e}{C_e} = \frac{(C_i - C_t)}{C_i} \times \frac{V}{M} \quad (14)$$

where C_i and C_t are the initial ion concentration, and final ion concentration of the solution, respectively, and M are the volumes of solution (mL) and amount of sorbent (g), respectively. The plot of $ln\ K_d$ versus $1/T$ gives a straight line, and the value of enthalpy change ΔH^o and entropy change ΔS^o can be calculated from the intercept and slope, respectively.

3. Results and Discussion

3.1. Batch experiment

The effects of contact time, the initial concentration, adsorbent dosage, pH and temperature on removal of NO_3^- were investigated.

3.2. Effect of pH solution and Zeta potential

The pH is one of the most critical factors controlling the ion-exchange process of nitrate onto modified clinoptilolite. To examine the effect of pH, the experiments were conducted by varying the pH values in the range of 2 – 12, the nitrate concentration of 25 mgL^{-1}, adsorbent dosage 5.0 g/100 mL, contact time 120 min. and the temperature of 30 ºC. The effect of pH on the removal of nitrate by clinoptilolite is shown in *Fig*. 1.

NO_3^- adsorption was found to increase with a decrease in the pH of the solution because a decrease

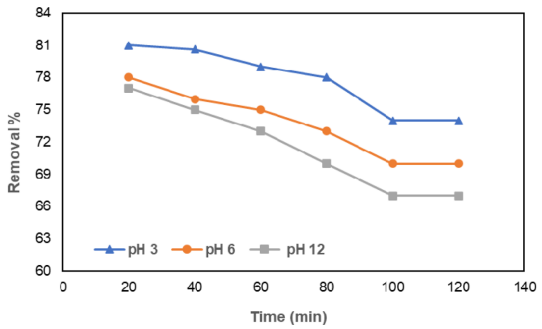

Fig. 1. Effect of pH on removal of nitrate.

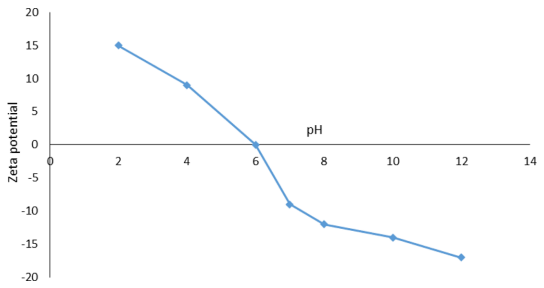

Fig. 2. Effect of pH on zeta potential of modified clinoptilolite.

in the pH of the solution (pH 3) resulted in more protons being available to protonate the chitosan amine group. This enhanced nitrate adsorption by modified clinoptilolite due to increased electrostatic interactions between chitosan's negatively charged nitrate group and a positively charged amine group. The surface charge of chitosan is positive in acidic pH, gradually decreases with increasing in pH, and has zero potential at pH 6. However, the adsorption at pH 6, where the surface charge of chitosan beads is neutral, maybe due to physical forces.[23] At pH levels above 6, an appreciable amount of nitrate adsorption by chitosan beads indicates the involvement of physical forces.[24] It is widely accepted that high pH significantly effects on the availability of NO_3^- as it influences nitrification and denitrification. Loss of NO_3^- to N_2O and NO emissions increase under low soil pH. The zeta potential describes the charging behavior at the solid-liquid interface.[25] The surface charge at the interface between clinoptilolite and the aqueous solution was measured.

The result is reported in *Fig.* 2 with a net zero charge at pH 6, meaning that the surface of clinoptilolite has a negative charge above this pH value, and the adsorption was easier to carry out. The zeta potential measurements revealed that the modified clinoptilolite surface has a negative charge in an aqueous solution at the investigated pH values (*Fig.* 2). The negative charge results from the Al^{3+} substitutions for Si^{4+} within the clinoptilolite lattice (isomorphic substitution), the broken bonds at the Si–O–Si generated at the particle surface during the grinding process, and the lattice imperfections. It is evident that the zeta potential of clinoptilolite, especially of the modified one, is strongly affected by the pH of the metal solution. In addition, the H^+ ions may be considered as exchangeable cations present in Si–OH and Al–OH. Therefore, the variation of pH of the solution in contact with the clinoptilolite is envisaged to affect the ion exchange process, controlled by electrostatic forces.[26]

3.3. Effect of initial concentration

The effect of initial concentration for nitrate removal was determined at the following conditions: nitrate concentration from 25 to 75 mgL^{-1}, the adsorbent dosage of 5.0 g/100 mL, contact time 120 minutes, and temperature of 30 °C. The removal adsorption increases with increasing the initial nitrate concentration, but the time required to reach equilibrium was independent of the initial nitrate concentration. The nitrate removal on modified clinoptilolite decreased from 82 % to 77 %, with increasing the initial concentration from 25 to 75 mgL^{-1}. For the lowest initial

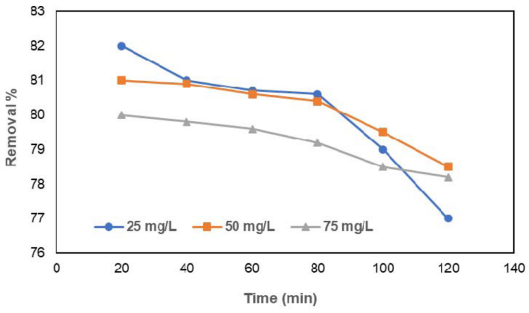

Fig. 3. Effect of initial concentration on removal of nitrate.

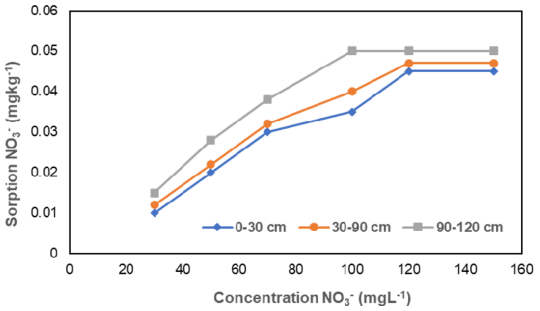

Fig. 4. Effect of initial NO_3^- concentration on NO_3^- sorption for 3 soil depths from a batch experiment using an iso-humic soil.

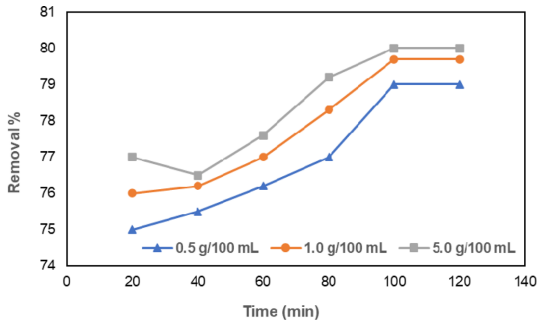

Fig. 5. Effect of adsorbent dosage on removal of nitrate.

concentrations, maximal removal reached 82 %, as shown in *Fig.* 3.

This may be attributed to the more active site available in sites. The initial NO_3^- concentration provides an important driving force to overcome the mass transfer limitations of NO_3^- between aqueous and solid phases. A higher initial NO_3^- concentration will increase the sorption process. The effect of initial NO_3^- concentration on NO_3^- sorption for all soil depths was investigated in the following concentrations (25, 50, 75, 100, 125, and 150 mg $NO_3^-L^{-1}$). *Fig.* 4 shows the change of the equilibrium sorption capacity of soil samples with different initial NO_3^- concentrations. It was observed that the amount of sorbed NO_3^- at equilibrium increased with increasing initial NO_3^- concentration for all soil horizons, although rates differed according to the soil layer. Many previous works reported that more NO_3^- is sorbed by the soil at low concentration than is left in solution. There is some controversy concerning the mechanism of NO_3^- adsorption at low concentrations in soil. On the contrary, the concentrations below 100 mg $NO_3^-L^{-1}$, NO_3^- sorption were low in the top horizon (0 – 30 cm), higher in the 30 – 90 cm horizon, and 90 – 120 cm depths. Between concentrations of 100 NO_3^- mgL^{-1} and 120 NO_3^- mgL^{-1}, the slope of the curves decreased. This decline in NO_3^- sorption with increased initial concentrations in all soil depths is likely due to the weakening of attractive forces between NO_3^- and the soil matrix and the desorption of other anions.

3.4. Effect of adsorbent dosage

The effect of adsorbent dosage on nitrate removal was a vigorous parameter influencing adsorption capacity and effluent concentration. The effect of adsorption dosage was studied at the following conditions: nitrate concentration 25 mgL^{-1}; adsorbent dosage 0.5 g/100 mL, 1.0 g/100 mL and 5.0 g/100 mL; temperature 30 °C and 120 minutes. The nitrate removal percentage increased from 75 % to 80 % with an increasing in adsorbent dosage from 0.5 to 5.0 g/100 mL, as depicted in *Fig.* 5.

The increase was attributed to the availability of active sites and high surface area at greater dosage.[28] The increase reaches equilibrium after 120 min, which may be due to the binding of almost all nitrate into clinoptilolite. The equilibrium established between the ions bound to the clinoptilolite suggested that the adsorption rate of nitrate from solution increases with an increase in the amount of adsorbent. The increase in the adsorbent dosage results in an increased adsorption percentage of nitrate. Increasing the adsorbent dosage increased the percentage removal of nitrate, which could be attributed to the increase in the adsorbent surface area of the adsorbent. *Fig.* 5 clearly shows that with an increasing amount of clinoptilolite indicating the dependence of adsorption upon the availability of binding sites for nitrate. The maximum removal of nitrate was observed at 80 % with a 5.0 g/100 mL adsorbent dosage.

3.5. Effect of contact time

The nitrate adsorption rate was rapid for the first

60 min and decreased over time. Equilibrium sorption was established after approximately 120 min for NO_3^- ions at an initial concentration of 100 mg/L. The results showed that the contact time required for maximum sorption of NO_3^- by different soil profiles was dependent on the initial NO_3^- concentration and specific soil components. This behavior suggests that at the initial stage, sorption takes place rapidly on the adsorbent's external surface, followed by a slower internal diffusion process, which may be the rate-determining step. This trend in NO_3^- sorption suggests that the binding may be through interactions with functional groups located on the surface of the soil. According to these results, the contact time was fixed at 120 min for the batch experiments to ensure that equilibrium was attained. The results demonstrated that the NO_3^- sorption was higher in deeper horizons at a fixed adsorbent dosage than in superficial horizons. The two deepest horizons contained more organic matter, which counterbalances the effect of positive charges of the oxides on NO_3^- sorption. Indeed, organic groups displace water ligands at the positively charged sites on surface oxides.[27] Kinetic studies for nitrate adsorption on natural clinoptilolite have been performed to determine the optimum adsorption contact time. The adsorption data obtained from this study reveals that nitrate adsorption increases with increasing contact time until the equilibrium is attained.

3.6. Effect of temperature

The effect of temperature was investigated at the following conditions: nitrate concentration 25 mgL^{-1}, adsorbent dosage 5.0 g/100 mL, and contact time 120 min. At higher temperature, the electrostatic interaction becomes weaker, which causes the anions to become smaller, promoting the adsorption of ions onto the surface of clinoptilolite with nitrate removal of 82 % at 30 °C (see *Fig.* 6). The adsorption removal decreased when the temperature was increased from 30 to 50 °C. This result indicates the exothermic nature of nitrate adsorption onto chitosan beads. A decrease in the nitrate uptake value with the temperature rise may be due to an increase in equilibrium concentration and finally achieving a saturated value. Experimental

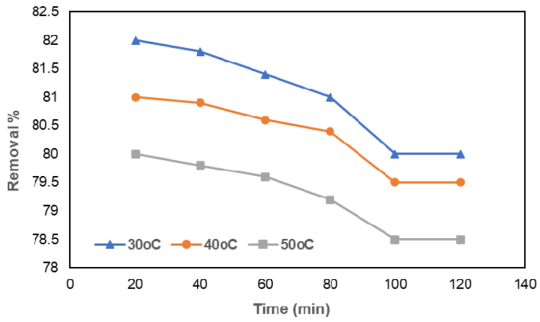

Fig. 6. Effect of Temperature on removal of nitrate.

results concerning the effect of temperature on NO_3^- adsorption on modified clinoptilolite are demonstrated in *Fig.* 6.

The temperature increases from 30 to 50 °C results in a decrease in NO_3^- adsorption. With increasing temperature, the attractive forces between the adsorbent surface and ions are weakened, which results in decreased adsorption.[29] On the other hand, the high adsorption at 30 and 50 °C occurs because increasing the temperature increases the rate of diffusion of adsorbate (physically adsorbed) across the external boundary layer and in the internal pores of the adsorbent particles. This could also be due to the retardation of processes such as the association of ions, aggregation of molecules, ion-pairing and complex formation in the system because of thermal agitation.[30] Results of temperature studies confirm that these materials responded positively to an increase in temperature concerning nitrate adsorption at 50 °C. The rise in temperature may change the properties of soil, such as pore size and carbon activity.

3.7. Adsorption isotherms

The initial and equilibrium adsorbate concentrations are important parameters that can affect the adsorption process considerably. Reviewing the results reported in *Figs.* 7 and 8, it can be found that an increase in NO_3^- concentration leads to an increase in its uptake.

Experimental results obtained for nitrate adsorption on clinoptilolite at 303 K have been fitted to the Langmuir adsorption model. The Langmuir constant (K_L) values, monolayer capacity of adsorbent (q_m), and R^2 are listed in *Table* 2.

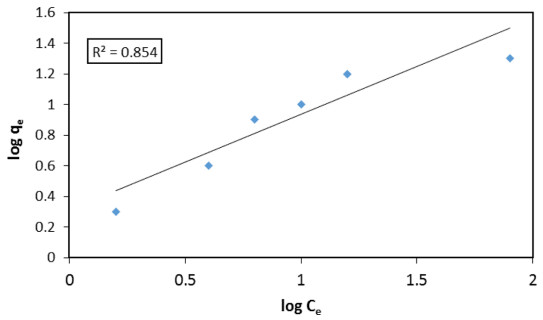

Fig. 7. Isotherm plots for the adsorption of nitrate onto clinoptilolite using the Langmuir isotherm.

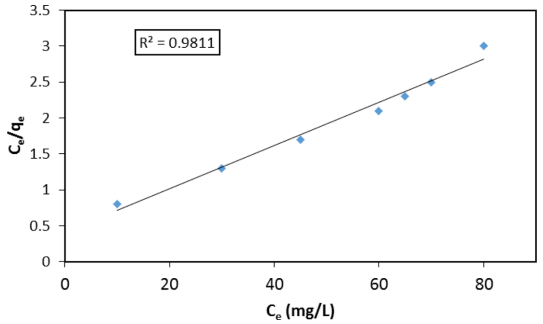

Fig. 8. Isotherm plots for the adsorption of nitrate onto clinoptilolite using the Freundlich isotherm.

High K_L values indicate the high affinity of modified clinoptilolite for nitrate adsorption. The R^2 values obtained confirm that the adsorption equilibrium data fitted well to the Langmuir model. This indicates uniform adsorption and strong nitrate-clinoptilolite interactions over adsorbent surfaces. Based on the Langmuir adsorption model, the predicted maximum monolayer nitrate adsorption capacity for clinoptilolite at 303K is found to be 125 mg/g. Moreover, modified clinoptilolite appears to be a better than chitosan adsorbent, carbon-based adsorbent, agricultural and industrial waste adsorbent, and various adsorbent.[30] The R_L parameter is considered a more reliable indicator for adsorption. The R_L value in *Table* 2 for nitrate adsorption on modified clinoptilolite is positive and less than unity (0.0714 < 1), indicating highly favorable adsorption.[30]

The Freundlich adsorption isotherm is the second most widely used mathematical description that characterizes adsorption capacity. This isotherm expresses the surface heterogeneity and the exponential distribution of active sites and their energies. The condition for a favourable adsorption process is 0.1 < *1/n* < 1.[30] The above condition is followed by *1/n* values, which indicate that nitrate adsorption on clinoptilolite is a favourable process. According to the statistical theory of adsorption, *1/n* < 1 implies a heterogeneous surface with minimal interactions between the adsorbed molecules or ions. The K_F values indicate that modified clinoptilolite has a good adsorption capacity for nitrate removal. This implies monolayer coverage of nitrate ions on the surface of chitosan beads. This would be reasonable given that the $-NH_2$ groups are the major functional groups in the adsorption process, and there is no interaction between sorbed nitrate ions due to the small size of nitrate ions compared to the distance between the amine groups of chitosan. Therefore, in this adsorption process, the use of the Langmuir isotherm model could be regarded as appropriate. The values of K_F, 1/*n*, and R^2 are given in *Table* 2. The high correlation coefficient (R^2 = 0.98) reflects that the experimental data agree well with the Langmuir adsorption model.

3.8. Kinetic studies

Adsorption kinetics is an important characteristic for evaluating the efficiency of adsorption. The kinetic behavior of this process was studied at pH 3 and 30 °C. In order to study the controlling mechanisms of the adsorption process, pseudo-first-order (Eq. (8)) and pseudo-second-order kinetic (Eq. (9)) rate models and an intra-particle diffusion model (Eq.

Table 2. Calculated isotherms parameters. Experimental conditions: pH = 6, T = 30 °C

	Langmuir Model		Freundlich Model		Dubinin-Raduskevich		
q_m	K_L	R_L	K_F	*1/n*	q_d	*K*	*E*
8.70	1.145	0.0714	1.562	0.568	8.27	9.15×10^{-9}	7.22

(10)) were used to test the experimental kinetic data.

Table 3 shows the parameters of three kinetic models chosen for this study. Comparison of the values of correlation coefficients (R^2 values) of the pseudo-first-order, pseudo-second-order and intra-particle diffusion models shows that the pseudo-second-order kinetic model best described the ammonium sorption data.

The studies done by Sharifnia *et al.* (2013) have shown that the kinetics of NO_3^- sorption follow the pseudo-second-order kinetic model. Sieczka and Koda (2016) suggested that the sorption mechanism is through intra-particle diffusion when the plot of q_t versus $t^{1/2}$ is multi-linear.[37] Our study shows that more than one process is undoubtedly responsible for the sorption of NO_3^- onto soils. Based on the coefficient of determination (R^2), it can be concluded that this model best described the sorption of NO_3^- onto soils. Considering the high values of R^2 for the pseudo-first-order and intra-particle diffusion models, we can assume that the sorption of NO_3^- can be additionally controlled by physical processes, surface, and pore-volume diffusion, respectively.[36]

Upon correlation of the kinetic data with the above two-rate models, it was found that both linear-form

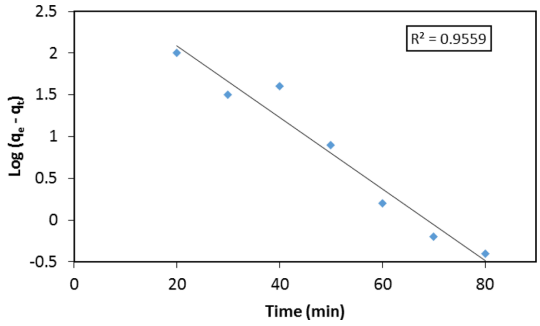

Fig. 9. Curve fit with a pseudo-first-order kinetic model.

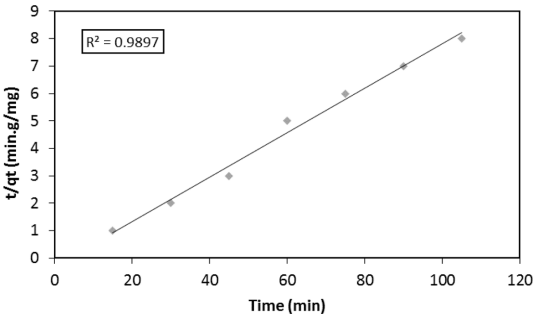

Fig. 10. Curve fit with a pseudo-second-order kinetic model.

plots using different initial nitrate concentrations give straight lines (*Fig.* 10). The lines for the pseudo-second-order rate model have higher correlation coefficients ($R^2 \approx 0.999$) compared to the correlation coefficient ($R^2 \approx 0.988$) obtained from the linear plot of the pseudo-first-order rate model. In this study, all of the kinetic data up to 120 min are used for modeling with the pseudo-second-order rate model, but for modeling with the pseudo-first-order rate model, only initial kinetic data (up to 120 min) have been used because the calculated values of q_e (cal) (mg/g) for all four initial concentrations of nitrate from the pseudo-first-order rate model using the whole range of contact time are physically unacceptable (e.g., lower q_e (cal) (mg/g) values were obtained from the higher initial concentration of nitrate ions). In many cases, the pseudo-first-order rate model does not fit well to the whole contact time range and is generally applicable over the initial stage of the adsorption processes.[24] *Table* 3 shows that the calculated and experimental equilibrium uptake values fit the pseudo-second-order rate model well, indicating that the pseudo-second-order reaction is better than the pseudo-first-order reaction.

The plot of q_t vs. $t^{0.5}$ (*Fig.* 11) using initial kinetic data up to 120 min has straight lines with correlation

Table 3. Kinetic parameters of different rate models

Pseudo-first-order			Pseudo-second-order			Intra-particle diffusion
$q_{e(exp)}$ (mg/g)	$q_{e(cal)}$ (mg/g)	k_1 (1/min)	$q_{e(cal)}$ (mg/g)	k_2 (g/mg.min)	h (mg/g.min)	k_p (mg/g/min0.5)
35.12	31.65	6.260×10^{-3}	38.02	2.020×10^{-4}	0.521	2.718

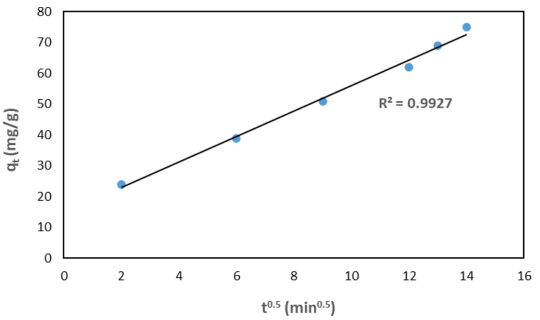

Fig. 11. Curve fit with intra-particle diffusion rate model kinetic model.

coefficients (R^2) ranging from 0.972 to 0.984. The linearity of the plots indicates that intraparticle diffusion might play a significant role in the initial stage of adsorption of nitrate on chitosan hydrobeads[24] because Eq. (9) is valid only for initial kinetic data. If the intra-particle diffusion is involved in the initial stage of the adsorption process, then the plot of q_t vs. $t^{0.5}$ would result in a linear relationship, and intra-particle diffusion would be the rate-controlling step if these lines have zero intercepts.[24] In the present study, the plot of q_t vs. $t^{0.5}$ (*Fig.* 11) for the initial kinetic data does not pass through the origin. Based on present data at initial adsorption, intra-particle diffusion is not the only rate controlling step for this adsorption process. The mechanism is simultaneous adsorption and intra-particle diffusion. *Table* 3 shows that the intra-particle diffusion rate constant (k_p) increases as the initial nitrate concentration increases because k_p is directly related to q_e and intra-particle diffusivity (D).

3.9. Thermodynamic parameters

Adsorption equilibrium constants (K) for varying temperatures have been used to evaluate the thermodynamic parameters of this adsorption process, and all the thermodynamic parameters of the adsorption process are shown in *Table* 4.

The values of the thermodynamic parameters (ΔG^o, ΔH^o, ΔS^o) given in *Table* 4 have been calculated using Eqs. (11)-(14). The negative ΔG^o values obtained reveal the thermodynamically feasible and spontaneous nitrate adsorption process. The higher negative value reflects more energetically favourable adsorption.[38] The Gibbs

Table 4. Thermodynamic parameters

Temperature (°C)	K	Thermodynamic Parameters		
		ΔG^o (kJ. mol^{-1})	ΔH^o (kJ.mol^{-1})	ΔS^o (kJ.mol^{-1}.K)
20	808.56	-16.232	-2.301	47.55
30	843.60	-17.004		48.52
40	764.08	-17.212		47.64
50	758.12	-17.735		47.78

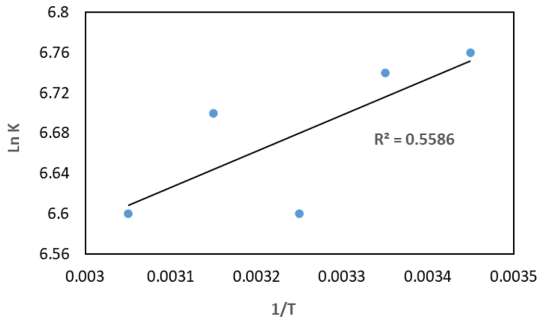

Fig. 12. *ln K* vs. 1/*T* for nitrate adsorption by chitosan.

free energy value at 50 °C is the highest negative value compared to the values of other temperatures. For that reason, more energetically favourable adsorption occurs at 50 °C.

The positive ΔH^o values indicate the endothermic nature of the adsorption process. If ΔH^o is constant, the plot of *ln K* vs. *1/T* gives a straight line whose slope equals $-\Delta H^o/R$ (*Fig.* 12). Generally, the enthalpy change due to chemisorption takes a value between 40 and 120 kJ/mol, which is more significance than that of physisorption. [39] Therefore, the low value of heat of adsorption (ΔH^o) obtained in this study indicates that adsorption is likely due to physisorption. The interaction between chitosan beads and nitrate ions is mainly electrostatic (Coulombic interactions). The heat of physical adsorption involves only relatively weak intermolecular forces such as van der Waals and mostly electrostatic interactions. The positive values of ΔS^o reflect the affinity of these adsorbents towards nitrate. They indicate that the randomness is increased at the solid/solution interface during the adsorption of nitrate onto chitosan hydrobeads and that significant changes occur in the internal structure of the adsorbent during adsorption.[40]

4. Conclusions

In this study, the effect of using clinoptilolite as soil amendments for the reduction of nitrate leaching from soil was examined. It was revealed that the pH 3, initial concentration of 25 mgL^{-1}, adsorbent dosage of 5.0 g/100 mL and temperature of 30 ^{o}C are the best removal conditions for nitrate. The Langmuir adsorption isotherm fit well to the equilibrium adsorption data. The kinetic adsorption parameters were proved to agree with the pseudo-second-order kinetic model. Intra-particle diffusion also plays a significant role at the initial stage of the adsorption process. The thermodynamics data demonstrated that the process behavior was spontaneous, randomness and endothermic. The results suggest that modification of clinoptilolite reduces the leaching of nitrate in soil.

Acknowledgements

The author thanks Vaal University of Technology for the support.

References

1. A. T. M. A. Choudhury and I. R. Kennedy, *Communications in Soil Science and Plant Analysis*, **36**, 1625-39 (2005).
2. A. R. B. Sofia, Y. Hala, A. T. Makkulawu, S. F. Hiola, H. Karim, R. N. Iriany, R. Sjahril and O. Jumadi, *Earth and Environ. Sci.*, **299**, 012017 (2019).
3. B. Azeem, K. Z. K. Shaari, Z. B. Man, A. Basit and T. H. Thanh, *J. Controlled Release*, **181**, 11-21 (2014).
4. M. S. Aulakh and S. S. Malhi, *Advances in Agronomy*, **86**, 341-409 (2005).
5. K. A. Nelson, S. M. Paniaguab and P. P. Motavallib, *Agronomy Journal Abstract Corn*., **101**, 681-687 (2008).
6. J. A. Ippolito, D. D. Tarkalson and G. A. Lehrsch, *Soil Science*, **176**, 136-142 (2011).
7. S. A. Abdulkareem, E. Muzenda, A. S. Afolabi and J. Kabuba, *Arab. J. Sc. Eng.,* **38**, 2263-2272 (2013).
8. A. Amankwah and J. Kabuba, *Life Sci. J*., **10**, 1012-1015 (2013).
9. A. Dziedzicka, B. Sulikowski and M. Ruggiero-Mikołajczyk, *Catalysis Today*, **259**, 50-58 (2016).
10. A. Mažeikienė, M. Valentukevičienė, A. M. Rimeik, A. B. Matuzevičius and R. Dauknys, *J. Environ. Eng. Landscape Manage*, **16**, 38-44 (2008).
11. A. Tressaud, *Advanced in Fluorine Science*, **2**, 1-286 (2006).
12. K. Margeta, N. Z. Logar, M. Šiljeg and A. Farkas, *IntechOpen*, 1-394 (2013).
13. Q. Hu, N. Chen, C. Feng and W. Hu, *Appl. Surface Sci*., **347**, 1-9 (2015).
14. E. Igberase, P. Osifo and A. Ofomaja, *Analytical Chemistry*, **2017**, Article ID 6150209 (2017).
15. L. Zong, F. Liu, D. Chen, X. Zhang, C. Ling and A. Li, *Chem. Eng. J*., **334**, 995-1005 (2018).
16. J. Zolgharnein, K. Dalvand, M. Rastgordani and P. Zolgharnein, *Alloys and Compounds*, **725**, 1006-1017 (2017).
17. S. N. do C. Ramos, A. L. P. Xavier, F. S. Teodoro, L. F. Gil and L. V. A. Gurgel, *Ind. Crops Prod*., **79**, 116-130 (2016).
18. A. S. Ozcan, B. Erden and A. Ozcan, *Colloids Surf. A*, **266**, 73-81(2005).
19. Y. S. Ho, *J. Hazard. Mater*., **136**, 681-689 (2006).
20. E. Fosso-Kankeu, *Physics and Chemistry of the Earth*, **105**, 170-176 (2018).
21. J. Xu, R. Koivula, W. Zhang, E. Wiikinkoski, S. Hietala and R. Harjula, *Hydrometallurgy*, **175**, 170-178 (2018).
22. A. A. Swelam, M. B. Awad, A. M. A. Salem and A. S. El-Feky, *Housing and Building National Research Center*, **78**, 1-9 (2016).
23. X. Xu, B. Gao, Y. Zhao, S. Chen, X. Tin, Q. Yue, J. Lin and Y. Wang, *J. Hazard Mater*, **203-204**, 86-92 (2012).
24. S. Chatterjee, D. S. Lee, M. W. Lee and S. H. Woo, S.H. *J. Hazard. Mater.*, **166**, 208-513 (2009).
25. K. Athanasiadis and B. Helmreich, *Water Res.*, **39**, 1527-1532 (2005).
26. S. Gupta and A. Kumar, *Appl. Water Sci*., **9**, 96 (2019).
27. W. Hamdi, F. Gamaoun, D. E. Pelster and M. Effen, *Applied and Environmental Soil Sci*., **2013**, Article ID 597824 (2013).
28. R. A. K. Rao and F Rehman, *J. Hazard. Mater.*, **181**, 405-412 (2010).
29. P. Sharma, G. Singh and R. Tomar, *J. Colloid Interface*

Sci., **332**, 298-308 (2009).
30. D. Bhardwaj, M. Sharma, P. Sharma and R. Tomar, *J. Hazard. Mater.*, **227-228**, 292-300 (2012).
31. H. D. Guan, E. Bestland, C. Y. Zhu, H. L. Zhu, D. Albertsdottir and J. Hutson, *J. Hazard. Mater.*, **183**, 616-621(2010).
32. H. Lin, Q. L. Liu, Y. B. Dong, Y. H. He and L. Wang, *Microporous Mesoporous Mater.*, **218**, 174-179 (2015).
33. J. Schick, P. Caullet and J. L. Paillaud, *Microporous Mesoporous Mater.*, **132**, 395-400 (2010).
34. Y. Zhan, Z. Zhu, J. Lin, Y. Qiu and J. Zhao, *J. Environ. Sci.*, **22**, 731-736 (2010).
35. S. Sharifnia, M. A. Khadivi, T. Shojaeimehr and Y. Shavisi, *J. Saudi Chem. Soc*., **20**, S342-S351 (2016).
36. A. Sieczka and E. Koda, *Appl. Sci.*, **6**(10), 269 (2016).
37. B. I. Olu-Owolabi, P. N. Diagboya and K. O. Adebowale, *J. Environ. Manag.*, **137**, 1-9 (2014).
38. Z. Aksu and E. Kabasakal, *Sep. Purif. Technol.*, **35**, 223-240 (2004).
39. M. Alkan, Ö. Demirbas, S. Celikcapa and M. Dogan, *J. Hazard. Mater*., **B116**, 135-145 (2004).
40. M. Mahramanlioglu, S. I. Kirbasalar and I. Kizilcikil, *Fresenius Environ. Bull*., **12**, 1483-1491 (2003).

Authors' Positions

John Kabuba : Professor